

A Unifying Generator Loss Function for Generative Adversarial Networks

Justin Veiner* Fady Alajaji† Bahman Ghahsifard‡

Abstract

A unifying α -parametrized generator loss function is introduced for a dual-objective generative adversarial network (GAN), which uses a canonical (or classical) discriminator loss function such as the one in the original GAN (VanillaGAN) system. The generator loss function is based on a symmetric class probability estimation type function, \mathcal{L}_α , and the resulting GAN system is termed \mathcal{L}_α -GAN. Under an optimal discriminator, it is shown that the generator's optimization problem consists of minimizing a Jensen- f_α -divergence, a natural generalization of the Jensen-Shannon divergence, where f_α is a convex function expressed in terms of the loss function \mathcal{L}_α . It is also demonstrated that this \mathcal{L}_α -GAN problem recovers as special cases a number of GAN problems in the literature, including VanillaGAN, Least Squares GAN (LSGAN), Least k th order GAN (LkGAN) and the recently introduced (α_D, α_G) -GAN with $\alpha_D = 1$. Finally, experimental results are conducted on three datasets, MNIST, CIFAR-10, and Stacked MNIST to illustrate the performance of various examples of the \mathcal{L}_α -GAN system.

1 Introduction

Generative adversarial networks (GANs), first introduced by Goodfellow *et al.* in 2014 [8], have a variety of applications in media generation [18], image restoration [26], and data privacy [12]. GANs aim to generate synthetic data that closely resembles the original real data with (unknown) underlying distribution $P_{\mathbf{x}}$. The GAN is trained such that the distribution of the generated data, $P_{\mathbf{g}}$, approximates $P_{\mathbf{x}}$ well. More specifically, low-dimensional random noise is fed to a generator neural network G to produce synthetic data. Real data and the generated data are then given to a discriminator neural network D scoring the data between 0 and 1, with a score close to 1 meaning that the discriminator

*Department of Mathematics and Statistics, Queen's University, Kingston, Ontario, Canada (justin.veiner@queensu.ca)

†Department of Mathematics and Statistics, Queen's University, Kingston, Ontario, Canada (fa@queensu.ca)

‡Department of Electrical and Computer Engineering, University of California, Los Angeles, CA, USA (ghahsifard@ucla.edu)

thinks the data belongs to the real dataset. The discriminator and generator play a minimax game, where the aim is to minimize the generator’s loss and maximize the discriminator’s loss.

Since their initial introduction, several variants of GAN have been proposed. The deep convolutional GAN (DCGAN) [27] utilizes the same loss functions as the VanillaGAN (the original GAN), combining GANs with convolutional neural networks, which are helpful when applying GANs to image data as they extract visual features from the data. DCGANs are more stable than the baseline model, but can suffer from mode collapse, which occurs when the generator learns that a select number of images can easily fool the discriminator, resulting in the generator only generating those images. Another notable issue with VanillaGAN is the tendency for the generator network’s gradients to vanish. In the early stages of training, the discriminator lacks confidence, assigning generated data values close to zero. Therefore, the objective function tends to zero, resulting in small gradients and a lack of learning. To mitigate this issue, a non-saturating generator loss function was proposed in [8] so that the gradients do not vanish early on in training.

In the original (VanillaGAN) problem setup, the objective function, expressed as a negative sum of two Shannon cross-entropies, is to be minimized by the generator and maximized by the discriminator. It is demonstrated that if the discriminator is fixed to be optimal (i.e. as a maximizer of the objective function), the GAN’s minimax game can be reduced to minimizing the Jensen-Shannon divergence (JSD) between the real and generated data’s probability distributions [8]. An analogous result was proven in [4] for RényiGANs, a dual-objective GAN using distinct discriminator and generator loss functions. More specifically, under a canonical discriminator loss function (as in [8]), and a generator loss function expressed in terms of two Rényi cross-entropies, it is shown that the RényiGAN optimization problem reduces to minimizing the Jensen-Rényi divergence, hence extending VanillaGAN’s result. Nowozin *et al.* formulated a class of loss functions in [24] parametrized by a lower semicontinuous convex function f , devising the f -GAN. However, the loss function can be tedious to derive, as it requires the computation of the Fenchel conjugate of f . The f -GAN problem minimizes an f -divergence. It can be shown that the f -GAN can interpolate between VanillaGAN, LSGAN, and HellingerGAN, among others [4, 8, 24, 29]. More recently, α -GAN was presented in [16], where the aim is to derive a class of loss functions parameterized by $\alpha > 0$, expressed in terms of a class probability estimation (CPE) loss between a real label $y \in \{0, 1\}$ and predicted label $\hat{y} \in [0, 1]$ [16]. The ability to control α as a hyperparameter is beneficial to be able to apply one system to multiple datasets, as two datasets may be optimal under different α values. This work was further analyzed in [17] and expanded in [31] to introduce the dual-objective (α_D, α_G) -GAN, which allowed for the generator and discriminator loss functions to have a distinct α parameter. When $\alpha_D = \alpha_G$, the α -GAN optimization reduces to minimizing an Arimoto divergence, as originally derived in [16]. Note that α -GAN can recover several f -GANs, such as HellingerGAN, VanillaGAN, and Total Variation GAN [16].

However, neither f -GAN nor α -GAN provide an analagous result to the JSD and Jensen-Rényi divergence minimizations for the VanillaGAN and RényiGAN problems, respectively, as they do not involve a Jensen-type divergence.¹

1.1 Contributions

The main objective of our work is to present a unifying approach that provides an axiomatic framework to encompass several existing GAN loss functions so that the GAN optimization can be simplified in terms of a Jensen-type divergence. In particular, our framework classifies the set of α -parameterized CPE-based loss functions \mathcal{L}_α , generalizing the work of [16], [17] and [31]. We then propose \mathcal{L}_α -GAN, a dual objective GAN that uses a function from this class for the generator, and uses any canonical discriminator loss function that admits the same optimizer as VanillaGAN [8]. We show that the minimax game played by these two loss functions is equivalent to the minimization of a Jensen- f_α -divergence, a Jensen-type divergence and another natural extension of the Jensen-Shannon divergence (in addition to the Jensen-Rényi divergence), where the generating function f_α of the divergence is directly computed from the CPE loss. This result can recover various prior dual-objective GAN results, thus unifying them under one parameterized generator loss function.

The rest of the paper is organized as follows. In Section 2, we review f -divergence measures and introduce the Jensen- f -divergence as an extension of the

Jensen-Shannon divergence. In Section 3, we establish our main result regarding the optimization of our unifying generator loss function, and show that our results can be applied to a large class of known GANs. We conduct experiments in Section 4 by implementing different manifestations of \mathcal{L}_α -GAN on three datasets, MNIST, CIFAR-10 and Stacked MNIST. Finally, we conclude the paper in Section 5.

2 Preliminaries

We begin by defining key information measures that will be used throughout the paper.

Definition 1 [1, 5, 6] *Let $f : [0, \infty) \rightarrow \mathbb{R}$ be a continuous convex function such that $f(1) = 0$. The **f -divergence** between two probability densities p and q with common support $\mathcal{R} \subseteq \mathbb{R}^d$ on the Lebesgue measurable space $(\mathcal{R}, \mathcal{B}(\mathcal{R}), \mu)$ is denoted by $D_f(p||q)$ and given by*

$$D_f(p||q) = \mathbb{E}_{\mathbf{A} \sim q} \left[f \left(\frac{p(\mathbf{A})}{q(\mathbf{A})} \right) \right] = \int_{\mathcal{R}} q f \left(\frac{p}{q} \right) d\mu, \quad (1)$$

¹By a Jensen-type divergence between distributions p and q , we mean the arithmetic average of two divergence measures, one between p and the mixture $\frac{p+q}{2}$, and the other between q and $\frac{p+q}{2}$.

where we have used the shorthand $\int_{\mathcal{R}} g d\mu := \int_{\mathcal{R}} g(x) d\mu(x)$, where g is a measurable function; we follow this convention from now on. We require that $f(1) = 0$ to satisfy the definiteness property of divergences, i.e., $D_f(p||q) = 0$ if and only if $p = q$ almost everywhere (a.e.). We present examples of f -divergences under various choices of their generating function f in Table 1. We will be invoking these divergence measures in different parts of the paper.

f -Divergence	Symbol	Formula	$f(u)$
Kullback-Leiber [15]	KL	$\int_{\mathcal{R}} p \log\left(\frac{p}{q}\right) d\mu$	$u \log u$
Jensen-Shannon [22]	JSD	$\frac{1}{2} \text{KL}\left(p \middle \frac{p+q}{2}\right) + \frac{1}{2} \text{KL}\left(q \middle \frac{p+q}{2}\right)$	$\frac{1}{2} (u \log u - (u+1) \log \frac{u+1}{2})$
Pearson χ^2 [23]	χ^2	$\int_{\mathcal{R}} \frac{(q-p)^2}{p} d\mu$	$\left(\sqrt{x} - \frac{1}{\sqrt{x}}\right)^2$
Pearson-Vajda ($k > 1$) [23]	$ \chi ^k$	$\int_{\mathcal{R}} \frac{ q-p ^k}{p^{\frac{k-1}{k}}} d\mu$	$u^{1-k} 1-u ^k$
Arimoto ($\alpha > 0, \alpha \neq 1$) [2, 19, 25]	\mathcal{A}_α	$\frac{\alpha}{\alpha-1} \left(\int_{\mathcal{R}} (p^\alpha + q^\alpha)^{\frac{1}{\alpha}} d\mu - 2^{\frac{1}{\alpha}} \right)$	$\frac{\alpha}{\alpha-1} \left((1+u)^{\frac{1}{\alpha}} - (1+u) - 2^{\frac{1}{\alpha}} + 2 \right)$
Hellinger ($\alpha > 0, \alpha \neq 1$) [10, 19]	\mathcal{H}_α	$\frac{1}{\alpha-1} (\int_{\mathcal{R}} p^\alpha q^{1-\alpha} d\mu - 1)$	$\frac{u^\alpha - 1}{\alpha - 1}$

Table 1: Examples of f -divergences.

The Rényi divergence of order α ($\alpha > 0, \alpha \neq 1$) between densities p and q and common support \mathcal{R} is used in [4] in the formulation of the RényiGAN problem. It is defined as [28, 30]

$$D_\alpha(p||q) = \frac{1}{\alpha - 1} \log \left(\int_{\mathcal{R}} p^\alpha q^{1-\alpha} d\mu \right). \quad (2)$$

Note that the Rényi divergence is not an f -divergence; however, it can be expressed as a transformation of the Hellinger divergence (which is itself an f -divergence):

$$D_\alpha(p||q) = \frac{1}{\alpha - 1} \log(1 + (\alpha - 1) \mathcal{H}_\alpha(p||q)). \quad (3)$$

We now introduce a new measure, the Jensen- f -divergence, which is analagous to the Jensen-Shannon and Jensen-Rényi divergences.

Definition 2 Let $f : [0, \infty) \rightarrow \mathbb{R}$ be a continuous convex function with $f(1) = 0$, and let $D_f(\cdot||\cdot)$ be its respective f -divergence. Then, the **Jensen- f -divergence** between two probability distributions p and q with common support $\mathcal{R} \subseteq \mathbb{R}$ on the Lebesgue measurable space $(\mathcal{R}, \mathcal{B}(\mathcal{R}), \mu)$ is denoted by $\text{JD}_f(p||q)$ and given by

$$\text{JD}_f(p||q) = \frac{1}{2} D_f \left(p \middle| \left| \frac{p+q}{2} \right| \right) + \frac{1}{2} D_f \left(q \middle| \left| \frac{p+q}{2} \right| \right), \quad (4)$$

where $D_f(\cdot||\cdot)$ is the f -divergence.

Remark 1 Examining (4), we note that the Jensen- f -divergence between p and q involves the f -divergences between either p or q and their mixture $(p+q)/2$. In other words to determine $\text{JD}_f(p||q)$, we only need $f\left(\frac{2p}{p+q}\right)$ and $f\left(\frac{2q}{p+q}\right)$ when taking the expectations in (1). Thus, it is sufficient to restrict the domain of the convex function f to the interval $[0, 2]$.

The next result shows that the Jensen-Shannon divergence is a Jensen- f -divergence.

Lemma 1 *Let p and q be two densities with common support $\mathcal{R} \subseteq \mathbb{R}$, and let $f : [0, \infty) \rightarrow \mathbb{R}$ be given by $f(u) = u \log u$. Then we have that*

$$\text{JD}_f(p||q) = \text{JSD}(p||q). \quad (5)$$

Proof 2 *We first note that f is continuous on $[0, \infty)$ and that $f(1) = 0$. Furthermore, we have that $f''(u) = \frac{1}{u}$, which is positive for $u > 0$. Therefore, f is also convex, and is a suitable function to construct a Jensen- f -divergence. We then have that*

$$\begin{aligned} \text{JSD}(p||q) &= \frac{1}{2} \text{KL} \left(p \middle| \middle| \frac{p+q}{2} \right) + \frac{1}{2} \text{KL} \left(q \middle| \middle| \frac{p+q}{2} \right) \\ &= \frac{1}{2} \int_{\mathcal{R}} p \log \left(\frac{2p}{p+q} \right) d\mu + \frac{1}{2} \int_{\mathcal{R}} q \log \left(\frac{2q}{p+q} \right) d\mu \\ &= \frac{1}{2} \int_{\mathcal{R}} \frac{p+q}{2} \left(\frac{2p}{p+q} \log \left(\frac{2p}{p+q} \right) \right) d\mu \\ &\quad + \frac{1}{2} \int_{\mathcal{R}} \frac{p+q}{2} \left(\frac{2q}{p+q} \log \left(\frac{2q}{p+q} \right) \right) d\mu \\ &= \text{JD}_f(p||q). \end{aligned}$$

3 Main Result

We now present our main result that unifies various generator loss functions under a CPE-based loss function \mathcal{L}_α for a dual-objective GAN, \mathcal{L}_α -GAN, with a canonical discriminator loss function that is optimized as in [8]. When some regularity conditions are satisfied, we show that under the optimal discriminator, our generator loss minimizes a Jensen- f -divergence.

Let $(\mathcal{X}, \mathcal{B}(\mathcal{X}), \mu)$ be the measure space of $n \times n \times m$ images (where $m = 1$ for black and white images and $m = 3$ for RGB images), and let $(\mathcal{Z}, \mathcal{B}(\mathcal{Z}), \mu)$ be a measure space such that $\mathcal{Z} \subseteq \mathbb{R}^d$. The discriminator neural network is given by $D : \mathcal{X} \rightarrow [0, 1]$, and the generator neural network is given by $G : \mathcal{Z} \rightarrow \mathcal{X}$. The generator's noise input is sampled from a multivariate Gaussian distribution $P_{\mathbf{z}} : \mathcal{Z} \rightarrow [0, 1]$. We denote the probability distribution of the real data by $P_{\mathbf{x}} : \mathcal{X} \rightarrow [0, 1]$ and the probability distribution of the generated data by $P_{\mathbf{g}} : \mathcal{X} \rightarrow [0, 1]$. We also set $P_{\mathbf{x}}$ and $P_{\mathbf{g}}$ as the densities corresponding to $P_{\mathbf{x}}$ and $P_{\mathbf{g}}$, respectively. We begin by introducing the \mathcal{L}_α -GAN system.

Definition 3 *For a fixed $\alpha \in \mathcal{A} \subseteq \mathbb{R}$, let $\mathcal{L}_\alpha : \{0, 1\} \times [0, 1] \rightarrow [0, \infty)$ such that \mathcal{L}_α is symmetric in the sense that*

$$\mathcal{L}_\alpha(1, \hat{y}) = \mathcal{L}_\alpha(0, 1 - \hat{y}), \quad \hat{y} \in [0, 1]. \quad (6)$$

The \mathcal{L}_α -GAN system is characterized by $(V_D, V_{\mathcal{L}_\alpha, G})$, where $V_D : \mathcal{X} \times \mathcal{Z} \rightarrow \mathbb{R}$ is the discriminator loss function, and $V_{\mathcal{L}_\alpha, G} : \mathcal{X} \times \mathcal{Z} \rightarrow \mathbb{R}$ is the generator

loss function, given by

$$V_{\mathcal{L}_\alpha, G}(D, G) = \mathbb{E}_{\mathbf{A} \sim P_{\mathbf{x}}}[-\mathcal{L}_\alpha(1, D(\mathbf{A}))] + \mathbb{E}_{\mathbf{B} \sim P_{\mathbf{g}}}[-\mathcal{L}_\alpha(0, D(\mathbf{B}))]. \quad (7)$$

Moreover, the \mathcal{L}_α -GAN problem is defined by

$$\sup_D V_D(D, G) \quad (8)$$

$$\inf_G V_{\mathcal{L}_\alpha, G}(D, G). \quad (9)$$

We now present our main result.

Theorem 3 For a fixed $\alpha \in \mathcal{A} \subseteq \mathbb{R}$ and $\mathcal{L}_\alpha : \{0, 1\} \times [0, 1] \rightarrow [0, \infty)$, let $(V_D, V_{\mathcal{L}_\alpha, G})$ be the loss functions of \mathcal{L}_α -GAN, and consider the joint optimization in (8)-(9). If V_D is a canonical loss function in the sense that it is maximized at $D = D^*$, where

$$D^* = \frac{P_{\mathbf{x}}}{P_{\mathbf{x}} + P_{\mathbf{g}}}, \quad (10)$$

then (9) reduces to

$$\inf_G V_{\mathcal{L}_\alpha, G}(D^*, G) = \inf_G 2a \text{JD}_{f_\alpha}(P_{\mathbf{x}} || P_{\mathbf{g}}) - 2ab, \quad (11)$$

where $\text{JD}_{f_\alpha}(\cdot || \cdot)$ is the Jensen- f_α -divergence, and $f_\alpha : [0, 2] \rightarrow \mathbb{R}$ is a continuous convex function satisfying $f_\alpha(1) = 0$ and

$$f_\alpha(u) = -u \left(\frac{1}{a} \mathcal{L}_\alpha \left(1, \frac{u}{2} \right) - b \right), \quad (12)$$

where $a, b \in \mathbb{R}$, $a \neq 0$. Finally, (11) is minimized when $P_{\mathbf{x}} = P_{\mathbf{g}}$ (a.e.).

Proof 4 Under the assumption that V_D is maximized at $D^* = \frac{P_{\mathbf{x}}}{P_{\mathbf{x}} + P_{\mathbf{g}}}$, we have that

$$\begin{aligned} V_{\mathcal{L}_\alpha, G}(D^*, G) &= \mathbb{E}_{\mathbf{A} \sim P_{\mathbf{x}}}[-\mathcal{L}_\alpha(1, D^*(\mathbf{A}))] + \mathbb{E}_{\mathbf{B} \sim P_{\mathbf{g}}}[-\mathcal{L}_\alpha(0, D^*(\mathbf{B}))] \\ &= - \int_{\mathcal{X}} P_{\mathbf{x}} \mathcal{L}_\alpha(1, D^*) d\mu - \int_{\mathcal{X}} P_{\mathbf{g}} \mathcal{L}_\alpha(0, D^*) d\mu \\ &= - \int_{\mathcal{X}} P_{\mathbf{x}} \mathcal{L}_\alpha \left(1, \frac{P_{\mathbf{x}}}{P_{\mathbf{x}} + P_{\mathbf{g}}} \right) d\mu - \int_{\mathcal{X}} P_{\mathbf{g}} \mathcal{L}_\alpha \left(0, \frac{P_{\mathbf{x}}}{P_{\mathbf{x}} + P_{\mathbf{g}}} \right) d\mu \\ &= -2 \int_{\mathcal{X}} \left(\frac{P_{\mathbf{x}} + P_{\mathbf{g}}}{2} \right) \frac{P_{\mathbf{x}}}{P_{\mathbf{x}} + P_{\mathbf{g}}} \mathcal{L}_\alpha \left(1, \frac{P_{\mathbf{x}}}{P_{\mathbf{x}} + P_{\mathbf{g}}} \right) d\mu \\ &\quad - 2 \int_{\mathcal{X}} \left(\frac{P_{\mathbf{x}} + P_{\mathbf{g}}}{2} \right) \frac{P_{\mathbf{g}}}{P_{\mathbf{x}} + P_{\mathbf{g}}} \mathcal{L}_\alpha \left(0, \frac{P_{\mathbf{x}}}{P_{\mathbf{x}} + P_{\mathbf{g}}} \right) d\mu \\ &\stackrel{(a)}{=} -2 \int_{\mathcal{X}} \left(\frac{P_{\mathbf{x}} + P_{\mathbf{g}}}{2} \right) \frac{P_{\mathbf{x}}}{P_{\mathbf{x}} + P_{\mathbf{g}}} \mathcal{L}_\alpha \left(1, \frac{P_{\mathbf{x}}}{P_{\mathbf{x}} + P_{\mathbf{g}}} \right) d\mu \end{aligned}$$

$$\begin{aligned}
& -2 \int_{\mathcal{X}} \left(\frac{P_{\mathbf{x}} + P_{\mathbf{g}}}{2} \right) \frac{P_{\mathbf{g}}}{P_{\mathbf{x}} + P_{\mathbf{g}}} \mathcal{L}_{\alpha} \left(1, \frac{P_{\mathbf{g}}}{P_{\mathbf{x}} + P_{\mathbf{g}}} \right) d\mu \\
& \stackrel{(b)}{=} -2 \int_{\mathcal{X}} \left(\frac{P_{\mathbf{x}} + P_{\mathbf{g}}}{2} \right) \frac{P_{\mathbf{x}}}{P_{\mathbf{x}} + P_{\mathbf{g}}} \left(\frac{-af_{\alpha} \left(\frac{2P_{\mathbf{x}}}{P_{\mathbf{x}} + P_{\mathbf{g}}} \right)}{\frac{2P_{\mathbf{x}}}{P_{\mathbf{x}} + P_{\mathbf{g}}}} + ab \right) d\mu \\
& \quad -2 \int_{\mathcal{X}} \left(\frac{P_{\mathbf{x}} + P_{\mathbf{g}}}{2} \right) \frac{P_{\mathbf{g}}}{P_{\mathbf{x}} + P_{\mathbf{g}}} \left(\frac{-af_{\alpha} \left(\frac{2P_{\mathbf{g}}}{P_{\mathbf{x}} + P_{\mathbf{g}}} \right)}{\frac{2P_{\mathbf{g}}}{P_{\mathbf{x}} + P_{\mathbf{g}}}} + ab \right) d\mu \\
& = 2a \left(\frac{1}{2} \int_{\mathcal{X}} \frac{P_{\mathbf{x}} + P_{\mathbf{g}}}{2} f_{\alpha} \left(\frac{2P_{\mathbf{x}}}{P_{\mathbf{x}} + P_{\mathbf{g}}} \right) d\mu \right. \\
& \quad \left. + \frac{1}{2} \int_{\mathcal{X}} \frac{P_{\mathbf{x}} + P_{\mathbf{g}}}{2} f_{\alpha} \left(\frac{2P_{\mathbf{g}}}{P_{\mathbf{x}} + P_{\mathbf{g}}} \right) d\mu \right) - 2ab \\
& = 2a \text{JD}_{f_{\alpha}}(P_{\mathbf{x}}||P_{\mathbf{g}}) - 2ab,
\end{aligned}$$

where:

- (a) holds since $\mathcal{L}_{\alpha}(1, u) = \mathcal{L}_{\alpha}(0, 1 - u)$ by (6), where $u = \frac{P_{\mathbf{x}}}{P_{\mathbf{x}} + P_{\mathbf{g}}}$.
- (b) holds by solving for $\mathcal{L}_{\alpha}(1, u)$ in terms of $f_{\alpha}(2u)$ in (12), where $u = \frac{P_{\mathbf{x}}}{P_{\mathbf{x}} + P_{\mathbf{g}}}$ in the first term and $u = \frac{P_{\mathbf{g}}}{P_{\mathbf{x}} + P_{\mathbf{g}}}$ in the second term.

Remark 5 Note that not only D^* given in (10) is an optimal discriminator of the (original) VanillaGAN discriminator loss function, but it also optimizes the LSGAN/LkGAN discriminator loss function when their discriminator's labels for fake and real data, γ and β , respectively satisfy $\gamma = 1$ and $\beta = 0$ (see Section 3.3).

We next show that the \mathcal{L}_{α} -GAN of Theorem 3 recovers as special cases a number of well-known GAN generator loss functions and their equilibrium points (under an optimal classical discriminator D^*).

3.1 VanillaGAN

VanillaGAN [8] uses the same loss function V_{VG} for both generator and discriminator, given by

$$V_{\text{VG}}(D, G) = \mathbb{E}_{\mathbf{A} \sim P_{\mathbf{x}}} [-\log D(\mathbf{A})] + \mathbb{E}_{\mathbf{B} \sim P_{\mathbf{g}}} [-\log(1 - D(\mathbf{B}))], \quad (13)$$

and can be cast as a saddle point optimization problem:

$$\inf_G \sup_D V_{\text{VG}}(D, G). \quad (14)$$

It is shown in [8] that the optimal discriminator for (14) is given by $D^* = \frac{P_{\mathbf{x}}}{P_{\mathbf{x}} + P_{\mathbf{g}}}$, as in (10). When $D = D^*$, the optimization reduces to minimizing the Jensen-Shannon divergence:

$$\inf_G V_{\text{VG}}(D^*, G) = \inf_G 2\text{JSD}(P_{\mathbf{x}}||P_{\mathbf{g}}) - 2\log 2. \quad (15)$$

We next show that (15) can be obtained from Theorem 3.

Lemma 2 *Consider the optimization of the VanillaGAN given in (14). Then we have that*

$$V_{\text{VG}}(D^*, G) = 2\text{JSD}(P_{\mathbf{x}}||P_{\mathbf{g}}) - 2\log 2 = V_{\mathcal{L}_{\alpha}, G}(D^*, G),$$

where $\mathcal{L}_{\alpha}(y, \hat{y}) = -y\log(\hat{y}) - (1-y)\log(1-\hat{y})$ for all $\alpha \in \mathcal{A} = \mathbb{R}$.

Proof 6 For any fixed $\alpha \in \mathbb{R}$, let the function \mathcal{L}_{α} in (7) be as defined in the statement:

$$\mathcal{L}_{\alpha}(y, \hat{y}) = -y\log(\hat{y}) - (1-y)\log(1-\hat{y}).$$

Note that \mathcal{L}_{α} is symmetric, since for $\hat{y} \in [0, 1]$, we have that

$$\mathcal{L}_{\alpha}(1, \hat{y}) = -\log(\hat{y}) = \mathcal{L}_{\alpha}(0, 1-\hat{y}).$$

We now derive f_{α} from \mathcal{L}_{α} using (12): setting $a = 1$ and $b = \log 2$, we have that

$$\begin{aligned} f_{\alpha}(u) &= -u \left(\frac{1}{a} \mathcal{L}_{\alpha} \left(1, \frac{u}{2} \right) - b \right) \\ &= -u \left(-\log \frac{u}{2} - \log 2 \right) \\ &= u \log u. \end{aligned}$$

Clearly f_{α} is continuous on $[0, \infty)$, and $f_{\alpha}(1) = 0$. Furthermore, we have that $f''(u) = \frac{1}{u} > 0$; hence, f_{α} is convex. By Lemma 1, we know that under the generating function $f(u) = u \log(u)$, the Jensen-f divergence reduces to the Jensen-Shannon divergence. Therefore, by Theorem 3, we have that

$$V_{\mathcal{L}_{\alpha}, G}(D^*, G) = 2a\text{JD}_{f_{\alpha}}(P_{\mathbf{x}}||P_{\mathbf{g}}) - 2ab = 2\text{JSD}(P_{\mathbf{x}}||P_{\mathbf{g}}) - 2\log 2 = V_{\text{VG}}(D^*, G).$$

3.2 α -GAN

The notion of α -GANs is introduced in [16] as a way to unify several existing GANs using a parameterized loss function. We describe α -GANs next.

Definition 4 [16] *Let $y \in \{0, 1\}$ be a binary label, $\hat{y} \in [0, 1]$, and fix $\alpha > 0$. The α -loss between y and \hat{y} is the map $\ell_{\alpha} : \{0, 1\} \times [0, 1] \rightarrow [0, \infty)$ given by*

$$\ell_{\alpha}(y, \hat{y}) = \begin{cases} \frac{\alpha}{\alpha-1} \left(1 - y\hat{y}^{\frac{\alpha-1}{\alpha}} + (1-y)(1-\hat{y})^{\frac{\alpha-1}{\alpha}} \right), & \alpha \in (0, 1) \cup (1, \infty) \\ -y\log \hat{y} - (1-y)\log(1-\hat{y}), & \alpha = 1. \end{cases} \quad (16)$$

Definition 5 [16] *For $\alpha > 0$, the α -GAN loss function is given by*

$$V_{\alpha}(D, G) = \mathbb{E}_{\mathbf{A} \sim P_{\mathbf{x}}}[-\ell_{\alpha}(1, D(\mathbf{A}))] + \mathbb{E}_{\mathbf{B} \sim P_{\mathbf{g}}}[-\ell_{\alpha}(0, D(\mathbf{B}))]. \quad (17)$$

The joint optimization of the α -GAN problem is given by

$$\inf_G \sup_D V_{\alpha}(D, G). \quad (18)$$

It is known that α -GAN recovers several well-known GANs by varying the α parameter, notably, the VanillaGAN ($\alpha = 1$) [8] and the HellingerGAN ($\alpha = \frac{1}{2}$) [24]. Furthermore, as $\alpha \rightarrow \infty$, V_α recovers a translated version of the WassersteinGAN loss function [3]. We now present the solution to the joint optimization problem presented in (18).

Proposition 7 [16] *Let $\alpha > 0$, and consider the joint optimization of the α -GAN presented in (18). The discriminator D^* that maximizes the loss function is given by*

$$D^* = \frac{P_{\mathbf{x}}^\alpha}{P_{\mathbf{x}}^\alpha + P_{\mathbf{g}}^\alpha}. \quad (19)$$

Furthermore, when $D = D^*$ is fixed, the problem in (18) reduces to minimizing an Arimoto divergence (as defined in Table 1) when $\alpha \neq 1$:

$$\inf_G V_\alpha(D^*, G) = \inf_G \mathcal{A}_\alpha(P_{\mathbf{x}} || P_{\mathbf{g}}) + \frac{\alpha}{\alpha - 1} \left(2^{\frac{1}{\alpha}} - 2 \right), \quad (20)$$

and a Jensen-Shannon divergence when $\alpha = 1$:

$$\inf_G V_1(D^*, G) = \inf_G \text{JSD}(P_{\mathbf{x}} || P_{\mathbf{g}}) - 2 \log 2, \quad (21)$$

where (20) and (21) achieve their minima if and only if $P_{\mathbf{x}} = P_{\mathbf{g}}$ (a.e.).

Recently, α -GAN was generalized in [31] to implement a dual objective GAN, which we recall next.

Definition 6 [31] *For $\alpha_D > 0$ and $\alpha_G > 0$, the (α_D, α_G) -GAN's **optimization** is given by*

$$\sup_D V_{\alpha_D}(D, G) \quad (22)$$

$$\inf_G V_{\alpha_G}(D, G) \quad (23)$$

where V_{α_D} and V_{α_G} are defined in (17), with α replaced by α_D and α_G respectively.

We now recall the solution to the (α_D, α_G) -GAN's optimization formulated in (22)-(23).

Proposition 8 [31] *Consider the joint optimization in (22)-(23). Let parameters $\alpha_D, \alpha_G > 0$ satisfy*

$$\left(\alpha_D \leq 1, \alpha_G > \frac{\alpha_D}{\alpha_D + 1} \right) \text{ or } \left(\alpha_D > 1, \frac{\alpha_D}{2} < \alpha_G \leq \alpha_D \right). \quad (24)$$

The discriminator D^ that maximizes V_{α_D} is given by*

$$D^* = \frac{P_{\mathbf{x}}^{\alpha_D}}{P_{\mathbf{x}}^{\alpha_D} + P_{\mathbf{g}}^{\alpha_D}}. \quad (25)$$

Furthermore, when $D = D^*$ is fixed, the minimization of V_{α_G} in (23) is equivalent to the following f -divergence minimization:

$$\inf_G V_{\alpha_G}(D^*, G) = \inf_G D_{f_{\alpha_D, \alpha_G}}(P_{\mathbf{x}} \| P_{\mathbf{g}}) + \frac{\alpha}{\alpha - 1} \left(2^{\frac{1}{\alpha}} - 2 \right), \quad (26)$$

where $f_{\alpha_D, \alpha_G} : [0, \infty) \rightarrow \mathbb{R}$ is given by

$$f_{\alpha_D, \alpha_G}(u) = \frac{\alpha_G}{\alpha_G - 1} \left(\frac{u^{\alpha_D(1 - \frac{1}{\alpha_G}) + 1} + 1}{(u^{\alpha_D} + 1)^{1 - \frac{1}{\alpha_G}}} \right). \quad (27)$$

We now apply the (α_D, α_G) -GAN to our main result in Theorem 3 by showing that (11) can recover (26) when $\alpha_D = 1$ (which corresponds to a VanillaGAN discriminator loss function).

Lemma 3 Consider the (α_D, α_G) -GAN given in Definition 6. Let $\alpha_D = 1$ and $\alpha_G = \alpha > \frac{1}{2}$. Then, the solution to (23) presented in Proposition 8 is equivalent to minimizing a Jensen- f_α -divergence: specifically, if D^* is the optimal discriminator given by (25), which is equivalent to (10) when $\alpha_D = 1$, then $V_{\alpha, G}(D^*, G)$ in (26) satisfies

$$V_{\alpha, G}(D^*, G) = 2^{\frac{1}{\alpha}} \text{JD}_{f_\alpha}(P_{\mathbf{x}} \| P_{\mathbf{g}}) + \frac{\alpha}{\alpha - 1} (2^{\frac{1}{\alpha}} - 2) = V_{\mathcal{L}_\alpha, G}(D^*, G), \quad (28)$$

where $\mathcal{L}_\alpha(y, \hat{y}) = \ell_\alpha(y, \hat{y})$ and

$$f_\alpha(u) = \frac{\alpha}{\alpha - 1} \left(u^{2 - \frac{1}{\alpha}} - u \right), \quad u \geq 0. \quad (29)$$

Proof 9 We want to show that Theorem 3 recovers Proposition 8. We set $\mathcal{L}_\alpha(y, \hat{y}) = \ell_\alpha(y, \hat{y})$. Note that ℓ_α is symmetric, since we have that

$$\ell_\alpha(1, \hat{y}) = \frac{\alpha}{\alpha - 1} (1 - \hat{y}^{1 - \frac{1}{\alpha}}) = \ell_\alpha(0, 1 - \hat{y}).$$

From Lemma 2, we know that when $\alpha = 1$, $f_\alpha(u) = u \log u$. For $\alpha \in (0, 1) \cup (1, \infty)$, setting $a = 2^{\frac{1}{\alpha} - 1}$ and $b = \frac{\alpha}{\alpha - 1} \left(2^{1 - \frac{1}{\alpha}} - 1 \right)$ in (12), we have that

$$\begin{aligned} f_\alpha(u) &= -u \left(\frac{1}{a} \mathcal{L}_\alpha \left(1, \frac{u}{2} \right) - b \right) \\ &= -u \left(2^{1 - \frac{1}{\alpha}} \frac{\alpha}{\alpha - 1} \left(1 - \left(\frac{u}{2} \right)^{1 - \frac{1}{\alpha}} \right) - \frac{\alpha}{\alpha - 1} (2^{1 - \frac{1}{\alpha}} - 1) \right) \\ &= \frac{\alpha}{\alpha - 1} (-u) [2^{1 - \frac{1}{\alpha}} - u^{1 - \frac{1}{\alpha}} - (2^{1 - \frac{1}{\alpha}} - 1)] \\ &= \frac{\alpha}{\alpha - 1} (u^{2 - \frac{1}{\alpha}} - u). \end{aligned}$$

Clearly $f_\alpha(1) = 0$. Furthermore for $\alpha \neq 1$, we have that

$$f_\alpha''(u) = \frac{(2\alpha - 1)u^{-\frac{1}{\alpha}}}{\alpha}, \quad u \geq 0,$$

which is positive for $\alpha > \frac{1}{2}$, and f_α is convex for $\alpha > \frac{1}{2}$. Therefore, by Theorem 3, we have that

$$\begin{aligned} V_{\mathcal{L}_{\alpha,G}}(D^*, G) &= 2a \text{JD}_{f_\alpha}(P_{\mathbf{x}} \| P_{\mathbf{g}}) - 2ab \\ &= 2 \cdot 2^{\frac{1}{\alpha}-1} \text{JD}_{f_\alpha}(P_{\mathbf{x}} \| P_{\mathbf{g}}) - 2 \frac{\alpha}{\alpha-1} 2^{\frac{1}{\alpha}-1} (2^{1-\frac{1}{\alpha}} - 1) \\ &= 2^{\frac{1}{\alpha}} \text{JD}_{f_\alpha}(P_{\mathbf{x}} \| P_{\mathbf{g}}) + \frac{\alpha}{\alpha-1} (2^{\frac{1}{\alpha}} - 2). \end{aligned}$$

We now show that the above Jensen- f_α -divergence is equal to the $f_{1,\alpha}$ -divergence originally derived for the $(1, \alpha)$ -GAN problem of Proposition 8 (note from Proposition 8, that if $\alpha_D = 1$, then $\alpha_G = \alpha > \frac{1}{2}$, so the range of α concurs with the range above required for the convexity of f_α). For any two distributions p and q with common support \mathcal{X} , we have that

$$\begin{aligned} D_{f_{1,\alpha}}(p \| q) &= \frac{\alpha}{\alpha-1} \int_{\mathcal{X}} q \frac{\left(\frac{p}{q}\right)^{2-\frac{1}{\alpha}} + 1}{\left(\frac{p}{q} + 1\right)^{1-\frac{1}{\alpha}}} d\mu - \frac{\alpha}{\alpha-1} 2^{\frac{1}{\alpha}} \\ &= \frac{\alpha}{\alpha-1} \int_{\mathcal{X}} q \frac{\left(\frac{p}{q}\right)^{2-\frac{1}{\alpha}} + 1}{\left(\frac{p+q}{q}\right)^{1-\frac{1}{\alpha}}} d\mu - \frac{\alpha}{\alpha-1} 2^{\frac{1}{\alpha}} \\ &= \frac{\alpha}{\alpha-1} \int_{\mathcal{X}} \left((p+q) \left(\frac{p}{p+q}\right)^{2-\frac{1}{\alpha}} + (p+q) \left(\frac{q}{p+q}\right)^{2-\frac{1}{\alpha}} \right) d\mu \\ &\quad - \frac{\alpha}{\alpha-1} 2^{\frac{1}{\alpha}} \\ &= \frac{\alpha}{\alpha-1} \frac{2}{2^{2-\frac{1}{\alpha}}} \int_{\mathcal{X}} \left(\frac{p+q}{2} \left(\frac{2p}{p+q}\right)^{2-\frac{1}{\alpha}} + \frac{p+q}{2} \left(\frac{2q}{p+q}\right)^{2-\frac{1}{\alpha}} \right) d\mu \\ &\quad - \frac{\alpha}{\alpha-1} 2^{\frac{1}{\alpha}} \\ &= \frac{\alpha}{\alpha-1} 2^{\frac{1}{\alpha}-1} \int_{\mathcal{X}} \left(\frac{p+q}{2} \left(\left(\frac{2p}{p+q}\right)^{2-\frac{1}{\alpha}} - \frac{2p}{p+q} \right) + p \right) d\mu \\ &\quad + \frac{\alpha}{\alpha-1} 2^{\frac{1}{\alpha}-1} \int_{\mathcal{X}} \left(\frac{p+q}{2} \left(\left(\frac{2q}{p+q}\right)^{2-\frac{1}{\alpha}} - \frac{2q}{p+q} \right) + q \right) d\mu \\ &\quad - \frac{\alpha}{\alpha-1} 2^{\frac{1}{\alpha}} \\ &= \frac{\alpha}{\alpha-1} 2^{\frac{1}{\alpha}} \frac{1}{2} \left(\int_{\mathcal{X}} \frac{p+q}{2} \left(\left(\frac{2p}{p+q}\right)^{2-\frac{1}{\alpha}} - \frac{2p}{p+q} \right) d\mu + 1 \right) \\ &\quad + \frac{\alpha}{\alpha-1} 2^{\frac{1}{\alpha}} \frac{1}{2} \left(\int_{\mathcal{X}} \frac{p+q}{2} \left(\left(\frac{2q}{p+q}\right)^{2-\frac{1}{\alpha}} - \frac{2q}{p+q} \right) d\mu + 1 \right) \\ &\quad - \frac{\alpha}{\alpha-1} 2^{\frac{1}{\alpha}} \end{aligned}$$

$$\begin{aligned}
&= 2^{\frac{1}{\alpha}} \text{JD}_{f_\alpha}(p||q) + \frac{\alpha}{\alpha-1} 2^{\frac{1}{\alpha}-1}(2) - \frac{\alpha}{\alpha-1} 2^{\frac{1}{\alpha}} \\
&= 2^{\frac{1}{\alpha}} \text{JD}_{f_\alpha}(p||q).
\end{aligned}$$

Therefore, $V_{\mathcal{L}_\alpha, G}(D^*, G) = V_\alpha(D^*, G)$.

Note that this lemma generalizes Lemma 2; the VanillaGAN is a special case of the $(1, \alpha)$ -GAN for $\alpha = 1$.

3.3 Shifted LkGANs and LSGANs

Least Squares GAN (LSGAN) was proposed in [21] to mitigate the vanishing gradient problem with VanillaGAN and to stabilize training performance. The LSGAN's loss function is derived from the squared error distortion measure, where we aim to minimize the distortion between the data samples and a target value we want the discriminator to assign the samples to. The LSGAN was generalized with the LkGAN in [4] by replacing the squared error distortion measure with the absolute error distortion measure of order $k \geq 1$, therefore introducing an additional degree of freedom to the generator's loss function. We first state the general LkGAN problem. We then apply the result of Theorem 3 to the loss functions of LSGAN and LkGAN.

Definition 7 [4] *Let $\gamma, \beta, c \in [0, 1]$ and let $k \geq 1$. The **LkGAN's loss functions**, denoted by $V_{\text{LSGAN}, D}$ and $V_{k, G}$ are given by*

$$V_{\text{LSGAN}, D}(D, G) = -\frac{1}{2} \mathbb{E}_{\mathbf{A} \sim P_{\mathbf{x}}}[(D(\mathbf{A}) - \beta)^2] - \frac{1}{2} \mathbb{E}_{\mathbf{B} \sim P_{\mathbf{g}}}[(D(\mathbf{B}) - \gamma)^2] \quad (30)$$

$$V_{k, G}(D, G) = \mathbb{E}_{\mathbf{A} \sim P_{\mathbf{x}}} [|D(\mathbf{A}) - c|^k] + \mathbb{E}_{\mathbf{B} \sim P_{\mathbf{g}}} [|D(\mathbf{B}) - c|^k]. \quad (31)$$

The **LkGAN problem** is the joint optimization

$$\sup_D V_{\text{LSGAN}, D}(D, G) \quad (32)$$

$$\inf_G V_{k, G}(D, G). \quad (33)$$

We next recall the solution to (32), which is a minimization of the Pearson-Vajda divergence $|\chi|^k(\cdot||\cdot)$ of order k (as defined in Table 1).

Proposition 10 [4] *Consider the joint optimization for the LkGAN presented in (32). Then, the optimal discriminator D^* that maximizes $V_{\text{LSGAN}, D}$ in (30) is given by*

$$D^* = \frac{\gamma P_{\mathbf{x}} + \beta P_{\mathbf{g}}}{P_{\mathbf{x}} + P_{\mathbf{g}}}. \quad (34)$$

Furthermore, if $D = D^*$, and $\gamma - \beta = 2(c - \beta)$, the minimization of $V_{k, G}$ in (31) reduces to

$$\inf_G V_{k, G}(D, G) = \inf_G |c - \beta|^k |\chi|^k(P_{\mathbf{x}} + P_{\mathbf{g}}||2P_{\mathbf{g}}). \quad (35)$$

Note that the LSGAN [21] is a special case of LkGAN, as we recover LSGAN when $k = 2$ [4].

By scrutinizing Proposition 10 and Theorem 3, we observe that the former cannot be recovered from the latter. However we can use Theorem 3 by slightly modifying the LkGAN generator's loss function. First, for the dual objective GAN proposed in Theorem 3, we need $D^* = \frac{P_{\mathbf{x}}}{P_{\mathbf{x}} + P_{\mathbf{g}}}$. By (34), this is achieved for $\gamma = 1$ and $\beta = 0$. Then, we define the intermediate loss function

$$\tilde{V}_{k,G}(D, G) = \mathbb{E}_{\mathbf{A} \sim P_{\mathbf{x}}} [|D(\mathbf{A}) - c_1|^k] + \mathbb{E}_{\mathbf{B} \sim P_{\mathbf{g}}} [|D(\mathbf{B}) - c_2|^k]. \quad (36)$$

Comparing the above loss function with (7), we note that setting $c_1 = 0$ and $c_2 = 1$ in (36) satisfies the symmetry property of \mathcal{L}_{α} . Finally, to ensure the generating function f_{α} satisfies $f_{\alpha}(1) = 0$, we shift each term in (36) by 1. Putting these changes together, we propose a revised generator loss function, denoted by $\hat{V}_{k,G}$, given by

$$\hat{V}_{k,G}(D, G) = \mathbb{E}_{\mathbf{A} \sim P_{\mathbf{x}}} [|D(\mathbf{A})|^k - 1] + \mathbb{E}_{\mathbf{B} \sim P_{\mathbf{g}}} [|1 - D(\mathbf{B})|^k - 1]. \quad (37)$$

We call a system that uses (37) as a generator loss function a **Shifted LkGAN (SLkGAN)**. If $k = 2$, we have a shifted version of the LSGAN generator loss function, which we call the **Shifted LSGAN (SLSGAN)**. Note that none of these modifications alter the gradients of $V_{k,G}$ in (31), since the first term is independent of G , the choice of c_1 is irrelevant, and translating a function by a constant does not change its gradients. However, from Proposition 10, for $\gamma = 0$, $\beta = 1$ and $c = 1$, we do not have that $\gamma - \beta = 2(c - \beta)$, and as a result, this modified problem does not reduce to minimizing a Pearson-Vajda divergence. Consequently, we can relax the condition on k in Definition 7 to just $k > 0$. We now show how Theorem 3 can be applied to \mathcal{L}_{α} -GAN using (37).

Lemma 4 *Let $k > 0$. Let V_D be a discriminator loss function, and let $\hat{V}_{k,G}$ be the generator's loss function defined in (37). Consider the joint optimization*

$$\sup_D V_D(D, G) \quad (38)$$

$$\inf_G \hat{V}_{k,G}(D, G) \quad (39)$$

If V_D is optimized at $D^ = \frac{P_{\mathbf{x}}}{P_{\mathbf{x}} + P_{\mathbf{g}}}$ (i.e., V_D is canonical), then we have that*

$$\hat{V}_{k,G}(D^*, G) = \frac{1}{2^{k-1}} \text{JD}_{f_k}(P_{\mathbf{x}} || P_{\mathbf{g}}) + \frac{1}{2^{k-1}} - \frac{1}{2},$$

where f_k is given by

$$f_k(u) = u(u^k - 1), \quad u \geq 0.$$

Examples of $V_D(D, G)$ that satisfy the requirements of Lemma 4 include the LkGAN discriminator loss function given by (30) with $\gamma = 1$ and $\beta = 0$, and the VanillaGAN discriminator loss function given by (13).

Proof 11 Let $k > 0$. We can restate the SLkGAN's generator loss function in (37) in terms of $V_{\mathcal{L}_{\alpha},G}$ in (7): we have that $V_{\mathcal{L}_{\alpha},G}(D^*, G) = \hat{V}_{k,G}(D^*, G)$, where $\alpha = k$ and $\mathcal{L}_k : \{0, 1\} \times [0, 1] \rightarrow [0, \infty)$ is given by

$$\mathcal{L}_k(y, \hat{y}) = -(y(\hat{y}^k - 1) + (1 - y)((1 - \hat{y})^k - 1)). \quad (40)$$

We have that \mathcal{L}_k is symmetric, since

$$\mathcal{L}_k(1, \hat{y}) = -(\hat{y}^k - 1) = \mathcal{L}_k(0, 1 - \hat{y}).$$

Furthermore, setting $a = \frac{1}{2^k}$ and $b = 2^k - 1$ in (12), we have that

$$\begin{aligned} f_k(u) &= -u \left(\frac{1}{a} \mathcal{L}_k \left(1, \frac{u}{2} \right) - b \right) \\ &= -u \left(2^k \left(1 - \left(\frac{u}{2} \right)^k \right) - (2^k - 1) \right) \\ &= -u(2^k - u^k - 2^k + 1) \\ &= u(u^k - 1). \end{aligned}$$

We clearly have that $f_k(1) = 0$ and that f_k is continuous. Furthermore, we have that $f_k''(u) = k(k+1)u$, which is positive for $u > 0$. Therefore f_k is convex. As a result, by Theorem 3, we have that

$$\begin{aligned} \hat{V}_{k,G}(D^*, G) &= \frac{1}{2^{k-1}} \text{JD}_{f_k}(P_{\mathbf{x}} || P_{\mathbf{g}}) - \frac{1}{2^{k-1}} (2^k - 1) \\ &= \frac{1}{2^{k-1}} \text{JD}_{f_k}(P_{\mathbf{x}} || P_{\mathbf{g}}) + \frac{1}{2^{k-1}} - \frac{1}{2}. \end{aligned}$$

We conclude this section by emphasizing that Theorem 3 serves as a unifying result recovering the existing loss functions in the literature and moreover, provides a way for generalizing new ones. Our aim in the next section is to demonstrate the versatility of this result in experimentation.

4 Experiments

We perform two experiments on three different image datasets which we describe below.

Experiment 1. In the first experiment, we compare the (α, α) -GAN with the $(1, \alpha)$ -GAN, controlling the value of α . Recall that $\alpha_D = 1$ corresponds to the canonical VanillaGAN (or DCGAN) discriminator. We aim to verify whether or not replacing an α -GAN discriminator with a VanillaGAN discriminator stabilizes or improves the system's performance depending on the value of α . Note that the result of Theorem 3 only applies to the (α_D, α_G) -GAN for $\alpha_D = 1$.

Experiment 2. We train two variants of $SLkGAN$, with the generator loss function as described in (37), parameterized by $k > 0$. We then utilize two different canonical discriminator loss functions to align with Theorem 3. The first is the VanillaGAN discriminator loss given by (13); we call the resulting dual objective GAN by **Vanilla-SLkGAN**. The second is the $LkGAN$ discriminator loss, given by (30), where we set $\alpha = 0$ and $\beta = 1$ such that the optimal discriminator is given by (10). We call this system by **Lk-SLkGAN**. We compare the two variants to analyze how the value of k and choice of discriminator loss impacts the system’s performance.

4.1 Experimental Setup

We run both experiments on three image datasets: MNIST [7], CIFAR-10 [14], and Stacked MNIST [20]. The MNIST dataset is a dataset of black and white handwritten digits between 0 and 9 of size $28 \times 28 \times 1$. The CIFAR-10 dataset is an RGB dataset of small images of common animals and modes of transportation of size $32 \times 32 \times 3$. The Stacked MNIST dataset is an RGB dataset derived from the MNIST dataset, constructed by taking three MNIST images, assigning each one of the three colour channels, and stacking the images on top of each other. The resulting images are then padded so that each one of them have size $32 \times 32 \times 3$.

For Experiment 1, we use α values of 0.5, 5.0, 10.0 and 20.0. For each value of α , we train the (α, α) -GAN and the $(1, \alpha)$ -GAN. We additionally train the DCGAN, which corresponds to the $(1, 1)$ -GAN. For Experiment 2, we use k values of 0.25, 1.0, 2.0, 7.5 and 15.0. Note that when $k = 2$, we recover LSGAN. For the MNIST dataset, we run 10 trials with the random seeds 123, 500, 1600, 199621, 60677, 20435, 15859, 33764, 79878, and 36123, and train each GAN for 250 epochs. For the RGB datasets (CIFAR-10 and Stacked MNIST), we run 5 trials with the random seeds 123, 1600, 60677, 15859, 79878, and train each GAN for 500 epochs. All experiments utilize an Adam optimizer for the stochastic gradient descent algorithm, with a learning rate of 2×10^{-4} , and parameters $\beta_1 = 0.5$, $\beta_2 = 0.999$ and $\epsilon = 10^{-7}$ [13]. We also experiment with the addition of a gradient penalty (GP); we add a penalty term to the discriminator’s loss function to encourage the discriminator’s gradient to have a unit norm [9].

The MNIST experiments were run on one 6130 2.1 GHz 1xV100 GPU, 8 CPUs, and 16 GB of memory. The CIFAR-10 and Stacked MNIST experiments were run on one Epyc 7443 2.8 GHz GPU, 8 CPUs and 16 GB of memory. For each experiment, we report the best overall Fréchet Inception Distance (FID) score [11], the best average FID score amongst all trials and its variance, and the average epoch the best FID score occurs and its variance. The FID score for each epoch was computed over 10 000 images. For each metric, the lowest numerical value corresponds to the model with the best metric (indicated in bold in the tables). We also report how many trials we include in our summary statistics, as it is possible for a trial to collapse and not train for the full num-

ber of epochs. The neural network architectures used in our experiments are presented in Appendix A. The training algorithms are presented in Appendix B.

4.2 Experimental Results

We report the FID metrics for Experiment 1 in Tables 2, 3 and 4, and for Experiment 2 in Tables 5, 6 and 7. We report only on those experiments that produced meaningful results. Models that utilize a simplified gradient penalty have the suffix “-GP”. We display the output of the best-performing (α_D, α_G) -GANs in Figure 1 and the best-performing SLKGANs in Figure 3. Finally, we plot the trajectory of the FID scores throughout training epochs in Figures 2 and 4.

(α_D, α_G) -GAN	Best FID score	Average best FID score	Best FID scores variance	Average epoch	Epoch variance	Number of successful trials (/10)
(1,0.5)-GAN	1.264	1.288	2.979×10^{-4}	227.25	420.25	4
(0.5,0.5)-GAN	1.209	1.265	0.001	234.5	156.7	6
(1,5)-GAN	1.125	1.17	8.195×10^{-4}	230.3	617.344	10
(1,10)-GAN	1.147	1.165	7.984×10^{-4}	225.6	253.156	10
(10,10)-GAN	36.506	39.361	16.312	1.5	0.5	2
(1,20)-GAN	1.135	1.174	0.001	237.5	274.278	10
(20,20)-GAN	33.23	33.23	0.0	1.0	0.0	1
DCGAN	1.154	1.208	0.001	231.3	357.122	10

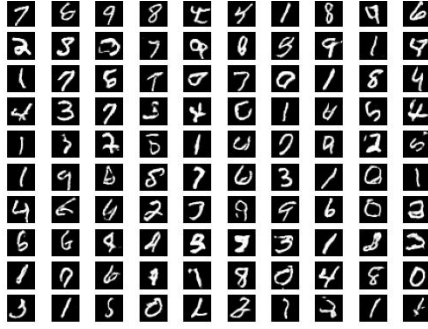
Table 2: (α_D, α_G) -GAN results for MNIST.

(α_D, α_G) -GAN	Best FID score	Average best FID score	Best FID scores variance	Average epoch	Epoch variance	Number of successful trials (/5)
(1,0.5)-GAN-GP	10.551	14.938	12.272	326.2	1808.7	5
(0.5,0.5)-GAN-GP	13.734	14.93	0.517	223.6	11378.3	5
(1,5)-GAN-GP	10.772	11.635	0.381	132.0	1233.5	5
(5,5)-GAN-GP	20.79	21.72	0.771	84.8	1527.2	5
(1,10)-GAN-GP	9.465	10.187	0.199	182.6	1096.3	5
(10,10)-GAN-GP	19.99	21.095	0.434	131.8	13374.7	5
(1,20)-GAN-GP	8.466	10.217	1.479	216.2	6479.7	5
(20,20)-GAN-GP	19.378	21.216	2.315	138.2	29824.2	5
DCGAN-GP	25.731	28.378	3.398	158.0	2510.5	5

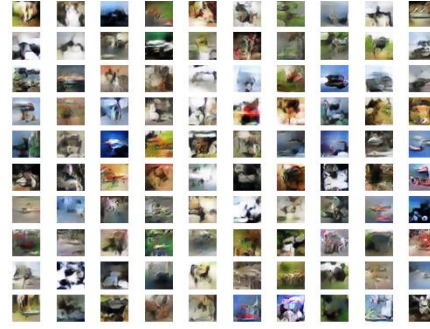
Table 3: (α_D, α_G) -GAN results for CIFAR-10.

(α_D, α_G) -GAN	Best FID score	Average best FID score	Best FID scores variance	Average epoch	Epoch variance	Number of succesful trials (/5)
(1,0.5)-GAN-GP	4.833	4.997	0.054	311.5	23112.5	2
(0.5,0.5)-GAN-GP	6.418	6.418	0.0	479.0	0.0	1
(1,5)-GAN-GP	7.98	7.988	1.357×10^{-4}	379.5	11704.5	2
(5,5)-GAN-GP	12.236	12.836	0.301	91.5	387.0	4
(1,10)-GAN-GP	7.502	7.528	0.001	326.5	14280.5	2
(10,10)-GAN-GP	14.22	14.573	0.249	95.0	450.0	2
(1,20)-GAN-GP	8.379	8.379	0.0	427.0	0.0	1
(20,20)-GAN-GP	16.584	16.584	0.0	94.0	0.0	1
DCGAN-GP	7.507	7.774	0.064	303.4	11870.8	5

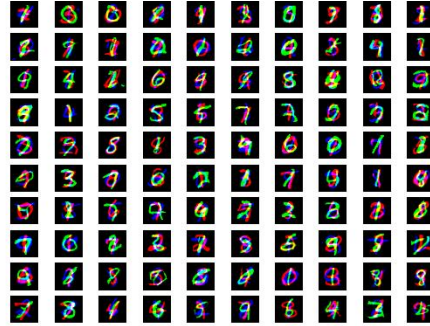
Table 4: (α_D, α_G) -GAN results for Stacked MNIST.



(a) (α_D, α_G) -GAN for MNIST, $\alpha_D = 1.0$, $\alpha_G = 5.0$, FID: 1.125.

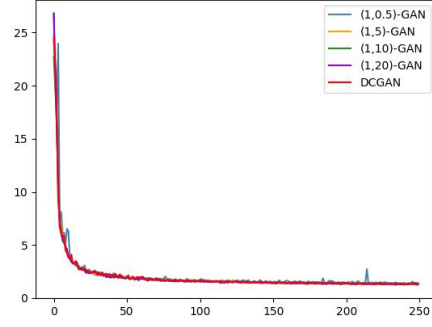


(b) (α_D, α_G) -GAN-GP for CIFAR-10, $\alpha_D = 1.0$, $\alpha_G = 20.0$, FID = 8.466.

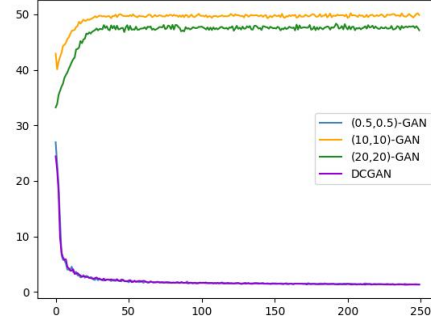


(c) (α_D, α_G) -GAN-GP for Stacked MNIST, $\alpha_D = 1.0$, $\alpha_G = 0.5$, FID = 4.833.

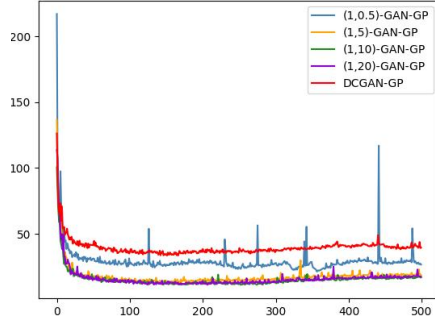
Figure 1: Generated images for the best-performing (α_D, α_G) -GANs.



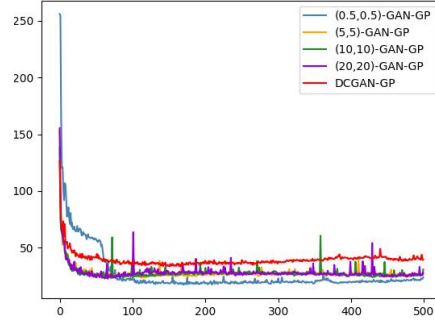
(a) $(1, \alpha)$ -GANs for MNIST.



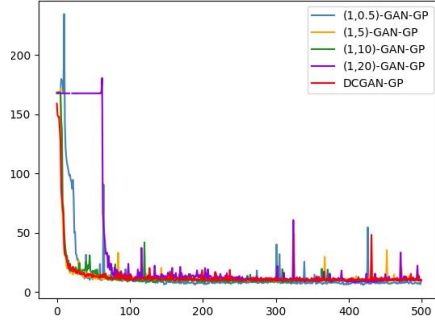
(b) (α, α) -GANs for MNIST



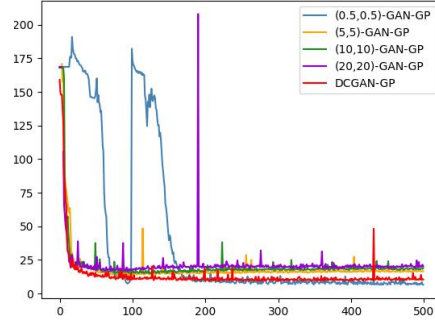
(c) $(1, \alpha)$ -GAN-GPs, for CIFAR-10.



(d) (α, α) -GAN-GPs for CIFAR-10.



(e) $(1, \alpha)$ -GAN-GPs for Stacked MNIST.



(f) (α, α) -GAN-GPs for Stacked MNIST.

Figure 2: Average FID scores vs. epochs for various (α_D, α_G) -GANs.

Variant-SLkGAN- k	Best FID score	Average best FID score	Best FID scores variance	Average epoch	Epoch variance	Number of successful trials (/10)
Lk-SLkGAN-0.25	1.15	1.174	6.298×10^{-4}	224.3	940.9	10
Vanilla-SLkGAN-0.25	1.112	1.162	0.001	237.0	124.0	10
Lk-SLkGAN-1.0	1.122	1.167	8.857×10^{-4}	233.0	124.0	10
Vanilla-SLkGAN-1.0	1.126	1.17	9.218×10^{-4}	226.2	1182.844	10
Lk-SLkGAN-2.0	1.148	1.198	5.248×10^{-4}	237.2	288.4	10
Vanilla-SLkGAN-2.0	1.124	1.184	8.933×10^{-4}	237.8	138.4	10
Lk-SLkGAN-7.5	1.455	1.498	4.422×10^{-4}	229.0	322.222	10
Vanilla-SLkGAN-7.5	1.439	1.511	0.001	212.2	1995.067	10
Lk-SLkGAN-15.0	1.733	1.872	0.005	198.8	1885.733	10
Vanilla-SLkGAN-15.0	1.773	1.876	0.005	171.6	3122.267	10
DCGAN	1.154	1.208	0.001	231.3	357.122	10

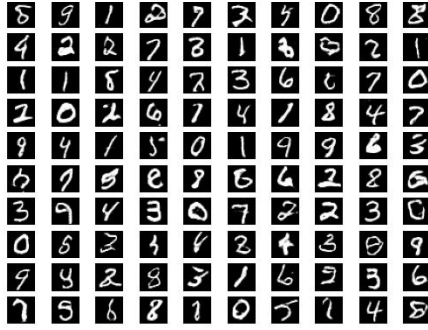
Table 5: SLkGAN results for MNIST.

Variant-SLkGAN- k	Best FID score	Average best FID score	Best FID scores variance	Average epoch	Epoch variance	Number of successful trials (/5)
Lk-SLkGAN-1.0	4.727	118.242	10914.643	60.8	1897.2	5
Vanilla-SLkGAN-1.0	4.821	5.159	0.092	88.0	506.5	5
Lk-SLkGAN-2.0	4.723	145.565	7492.26	73.2	3904.2	5
Vanilla-SLkGAN-2.0	4.58	5.1	0.261	105.4	740.8	5
Lk-SLkGAN-7.5	6.556	155.497	7116.521	254.6	18605.3	5
Vanilla-SLkGAN-7.5	6.384	48.905	8698.195	72.2	1711.7	5
Lk-SLkGAN-15.0	8.576	145.774	5945.097	263.0	36463.0	5
Vanilla-SLkGAN-15.0	7.431	50.868	8753.002	82.6	3106.8	5
DCGAN	4.753	5.194	0.117	88.6	462.8	5
Lk-SLkGAN-0.25-GP	17.366	18.974	2.627	87.8	1897.2	5
Vanilla-SLkGAN-0.25-GP	16.013	17.912	1.961	189.0	9487.5	5
Lk-SLkGAN-1.0-GP	10.771	12.567	1.083	77.8	239.2	5
Vanilla-SLkGAN-1.0-GP	8.569	9.588	0.749	197.6	2690.3	5
Lk-SLkGAN-2.0-GP	23.11	25.013	1.924	75.4	658.8	5
Vanilla-SLkGAN-2.0-GP	28.215	29.69	1.242	232.0	20438.5	5
Lk-SLkGAN-7.5-GP	33.304	41.48	49.187	82.8	1081.2	5
Vanilla-SLkGAN-7.5-GP	33.085	34.799	1.597	290.8	12714.7	5
Lk-SLkGAN-15.0-GP	9.157	12.504	3.839	310.4	6976.8	5
Vanilla-SLkGAN-15.0-GP	7.283	8.568	1.535	185.6	5978.3	5
DCGAN-GP	25.731	28.378	3.398	158.0	2510.5	5

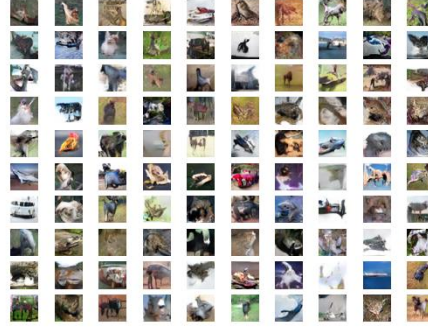
Table 6: SLkGAN results for CIFAR-10.

Variant-SLkGAN- k	Best FID score	Average best FID score	Best FID scores variance	Average epoch	Epoch variance	Number of successful trials (/5)
Lk-SLkGAN-0.25-GP	10.541	11.824	0.678	113.6	356.3	5
Vanilla-SLkGAN-0.25-GP	5.197	5.197	0.0	496.0	0.0	1
Lk-SLkGAN-1.0-GP	11.545	12.046	0.291	89.0	238.5	5
Vanilla-SLkGAN-1.0-GP	7.475	7.626	0.045	177.0	3528.0	2
Lk-SLkGAN-2.0-GP	10.682	12.782	2.12	180.2	28484.7	5
Vanilla-SLkGAN-2.0-GP	6.023	7.096	0.991	416.667	12244.333	3
Lk-SLkGAN-7.5-GP	8.912	9.906	0.577	239.0	35663.5	5
Vanilla-SLkGAN-7.5-GP	6.074	6.43	0.164	238.0	21729.5	5
Lk-SLkGAN-15.0-GP	4.458	4.74	0.029	253.4	11512.3	5
Vanilla-SLkGAN-15.0-GP	3.836	3.873	0.002	485.0	354.667	4
DCGAN-GP	7.507	7.774	0.064	303.4	11870.8	5

Table 7: SLkGAN results for Stacked MNIST.



(a) Vanilla-SLkGAN-0.25 for MNIST, FID = 1.112.

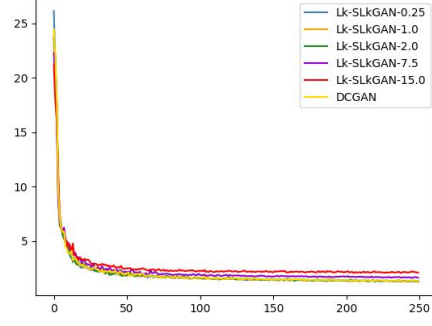


(b) Vanilla-SLkGAN-2.0 for CIFAR-10, FID = 4.58.

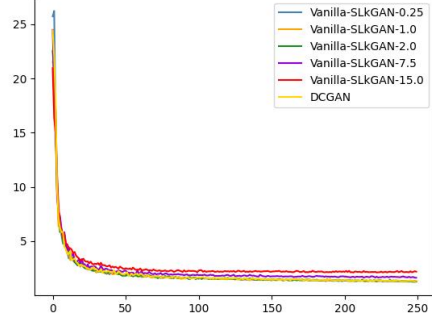


(c) Vanilla-SLkGAN-15.0-GP for Stacked MNIST, FID = 3.836.

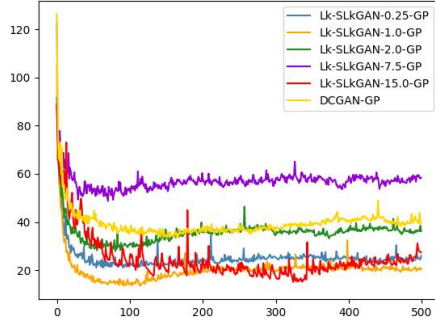
Figure 3: Generated images for best-performing SLkGANs.



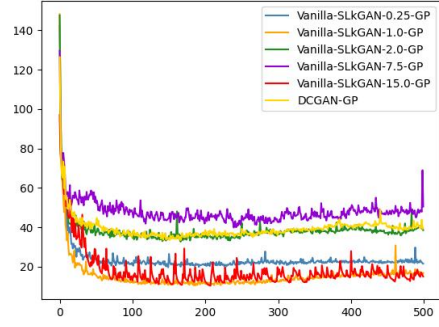
(a) Lk -SLkGANs for MNIST.



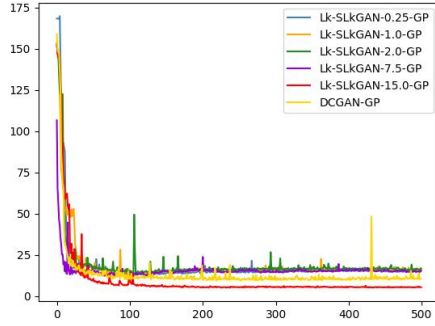
(b) Vanilla-SLkGANs for MNIST.



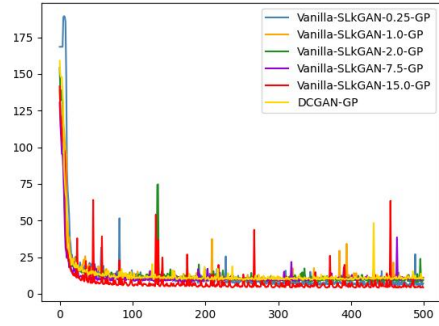
(c) Lk -SLkGAN-GPs for CIFAR-10.



(d) Vanilla-SLkGAN-GPs for CIFAR-10.



(e) Lk -SLkGAN-GPs for Stacked MNIST.



(f) Vanilla-SLkGAN-GPs, Stacked MNIST.

Figure 4: FID scores vs. epochs for various SLkGANs.

4.3 Discussion

4.3.1 Experiment 1

From Table 2, we note that 37 of the 90 trials collapse before 250 epochs have passed without a gradient penalty. The (5,5)-GAN collapses for all 5 trials, and hence it is not displayed in Table 2. This behaviour is expected, as the (α, α) -GAN is more sensitive to exploding gradients when α does not tend to 0 or $+\infty$ [16]. The addition of a gradient penalty could mitigate the discriminator’s gradients diverging in the (5,5)-GAN by encouraging gradients to have a unit norm. Using a VanillaGAN discriminator with an α -GAN generator (i.e., the $(1, \alpha)$ -GAN) produces better quality images for all tested values of α , compared to when both networks utilize an α -GAN loss function. The (1,10)-GAN achieves excellent stability, converging in all 10 trials, and also achieves the lowest average FID score. The (1,5)-GAN achieves the lowest FID score overall, marginally outperforming DCGAN.

Likewise, for the CIFAR-10 and Stacked MNIST datasets, the $(1, \alpha)$ -GAN produces lower FID scores than the (α, α) -GAN (see Tables 3 and 4). However, both models are more stable with the CIFAR-10 dataset. With the exception of DCGAN, no model converged to its best FID score for all 5 trials with the Stacked MNIST dataset. Comparing the trials that did converge, both (α, α) -GAN and $(1, \alpha)$ -GAN performed better on the Stacked MNIST dataset than the CIFAR-10 dataset. For CIFAR-10, the (1,10)- and (1,20)-GANs produced the best overall FID score and the best average FID score respectively. On the other hand, the (1,0.5)- α -GAN produced the best overall FID score and the best average FID score for the Stacked MNIST dataset. We also observe a tradeoff between speed and performance for the CIFAR-10 and Stacked MNIST datasets: the $(1, \alpha)$ -GANs arrive at their lowest FID scores later than their respective (α, α) -GANs, but achieve lower FID scores overall.

Comparing Figures 2c and 2d, we observe that the (α, α) -GAN-GP provides more stability than the $(1, \alpha)$ -GAN for lower values of α (i.e. $\alpha = 0.5$), while the $(1, \alpha)$ -GAN-GP exhibits more stability for higher α values ($\alpha = 10$ and $\alpha = 20$). Figures 2e and 2f show that the two α -GANs trained on the Stacked MNIST dataset exhibit unstable behaviour earlier into training when $\alpha = 0.5$ or $\alpha = 20$. However, both systems stabilize and converge to their lowest FID scores as training progresses. The (0.5,0.5)-GAN-GP system in particular exhibits wildly erratic behaviour for the first 200 epochs, then finishes training with a stable trajectory that outperforms DCGAN-GP.

A future direction is to explore how the complexity of an image dataset influences the best choice of α . For example, the Stacked MNIST dataset might be considered to be less complex than CIFAR-10, as images in the Stacked MNIST dataset only contain four unique colours (black, red, green, and blue), while the CIFAR-10 dataset utilizes significantly more colours.

4.3.2 Experiment 2

We see from Table 5 that all Lk - Lk GANs and Vanilla- SLk GANs have FID scores comparable to the DCGAN. When $k = 15$, Vanilla- SLk GAN and Lk - SLk GAN arrive at their lowest FID scores slightly earlier than DCGAN and other SLk GANs.

The addition of a simplified gradient penalty is necessary for Lk - SLk GAN to achieve overall good performance on the CIFAR-10 dataset (see Table 6). Interestingly, Vanilla- SLk GAN achieves lower FID scores without a gradient penalty for lower k values ($k = 1, 2$), and with a gradient penalty for higher k values ($k = 7.5, 15$). When $k = 0.25$, both SLk GANs collapsed for all 5 trials without a gradient penalty.

Table 7 shows that Vanilla- SLk GANs achieve better FID scores than their respective Lk - Lk GAN counterparts. However, Vanilla- SLk GANs are more stable, as no single trial collapsed, while 10 of the 25 Vanilla- SLk GAN trials collapsed before 500 epochs had passed. While all Vanilla- SLk GANs outperform the DCGAN with gradient penalty, Lk - SLk GAN-GP only outperforms DCGAN-GP when $k = 15$. Except for when $k = 7.5$, we observe that the Lk - SLk GAN takes less epochs to arrive at its lowest FID score. Comparing Figures 4e and 4f, we observe that the Lk - SLk GANs exhibit more stable FID score trajectories than their respective Vanilla- SLk GANs. This makes sense, as the Lk GAN loss function aims to increase the GAN’s stability compared to DCGAN [4].

5 Conclusion

We introduced a parameterized CPE-based generator loss function for a dual-objective GAN termed \mathcal{L}_α -GAN which, when used in tandem with a canonical discriminator loss function that achieves its optimum in (10), minimizes a Jensen- f_α -divergence. We showed that this system can recover VanillaGAN, $(1, \alpha)$ -GAN, and Lk GAN as special cases. We conducted experiments with the three aforementioned \mathcal{L}_α -GANs on three image datasets. The experiments indicate that $(1, \alpha)$ -GAN exhibits better performance than (α_D, α) -GAN with $\alpha_D > 1$. They also show that the devised SLk GAN system achieves lower FID scores and more stability with a VanillaGAN discriminator compared with an Lk GAN discriminator. Future work includes finding more examples of existing GANs that fall under our result. Additionally, one can attempt to apply the \mathcal{L}_α -GAN to a general judiciously designed CPE loss \mathcal{L}_α and evaluate that model’s performance.

A Neural Network Architectures

We outline the architectures used for the generator and discriminator. For the MNIST dataset, we use the architectures of [4]. For the CIFAR-10 and Stacked MNIST datasets, we base the architectures on [27]. We summarize some aliases for the architectures in Table 8. For all models we use a batch size of 100 and

noise size of 784 for the generator input.

Alias	Definition
FC	Fully Connected
UpConv2D	Deconvolutional Layer
Conv2D	Convolutional Layer
BN	Batch Normalization
LeakyReLU	Leaky Rectified Linear Unit

Table 8: Summary of aliases used to describe neural network architectures.

We omit the bias in the convolutional and deconvolutional layers to decrease the number of parameters being trained, which in turn decreases computation times. We initialize our kernels using a normal distribution with zero mean and variance 0.01. We present the MNIST architectures in Tables 9 and 10, and the CIFAR-10 and Stacked MNIST architectures in Tables 11 and 12.

Layer	Output Size	Kernel	Stride	BN	Activation
Input	$28 \times 28 \times 1$	No			
Conv2D	$14 \times 14 \times 64$	5×5	2	No	LeakyReLU(0.3)
Dropout(0.3)				No	
Conv2D	$7 \times 7 \times 128$	5×5	2	No	LeakyReLU(0.3)
Dropout(0.3)				No	
FC	1			No	Sigmoid

Table 9: Discriminator architecture for the MNIST dataset.

Layer	Output Size	Kernel	Stride	BN	Activation
Input	784				
FC	$7 \times 7 \times 256$				
UpConv2D	$7 \times 7 \times 128$	5×5	1	Yes	LeakyReLU(0.3)
UpConv2D	$14 \times 14 \times 64$	5×5	2	Yes	LeakyReLU(0.3)
UpConv2D	$28 \times 28 \times 1$	5×5	2	No	Tanh

Table 10: Generator architecture for the MNIST dataset

Layer	Output Size	Kernel	Stride	BN	Activation
Input	$32 \times 32 \times 3$				
Conv2D	$16 \times 16 \times 128$	3×3	2	No	LeakyReLU(0.2)
Conv2D	$8 \times 8 \times 128$	3×3	2	No	LeakyReLU(0.2)
Conv2D	$4 \times 4 \times 256$	3×3	2	No	LeakyReLU(0.2)
Dropout(0.4)				No	
FC	1				Sigmoid

Table 11: Discriminator architecture for the CIFAR-10 and Stacked MNIST datasets.

Layer	Output Size	Kernel	Stride	BN	Activation
Input	784				
FC	$4 \times 4 \times 256$				
UpConv2D	$8 \times 8 \times 128$	4×4	2	Yes	LeakyReLU(0.2)
UpConv2D	$16 \times 16 \times 128$	4×4	2	Yes	LeakyReLU(0.2)
UpConv2D	$32 \times 32 \times 128$	4×4	2	Yes	LeakyReLU(0.2)
Conv2D	$32 \times 32 \times 3$	3×3	1	No	Tanh

Table 12: Generator architecture for the CIFAR-10 and Stacked MNIST datasets.

B Algorithms

We outline the algorithms used to train our models in Algorithms 1, 2 and 3.

Algorithm 1 Overview of (α_D, α_G) -GAN training

Require α_D, α_G , Number of epochs n_e , Batch size B , Learning rate η
Initialize Generator G with parameters θ_G , Discriminator D with parameters θ_D .
for $i = 1$ to n_e **do**
 Sample batch of real data $\mathbf{x} = \{\mathbf{x}_1, \dots, \mathbf{x}_B\}$ from dataset
 Sample batch of Gaussian noise vectors $\mathbf{z} = \{\mathbf{z}_1, \dots, \mathbf{z}_B\} \sim \mathcal{N}(\mathbf{0}, \mathbf{I})$
 Update the discriminator's parameters using an Adam optimizer with learning rate η by descending the gradient:

$$\nabla_{\theta_D} \left(-\frac{1}{B} \sum_{i=1}^B (-\ell_\alpha(1, D(\mathbf{x}_i)) - \ell_\alpha(0, D(G(\mathbf{z}_i)))) \right)$$

or **update** the discriminator's parameters with a simplified GP:

$$\begin{aligned} \nabla_{\theta_D} \left(-\frac{1}{B} \sum_{i=1}^B (-\ell_\alpha(1, D(\mathbf{x}_i)) - \ell_\alpha(0, D(G(\mathbf{z}_i)))) \right) \\ + 5 \left(\sum_{i=1}^B \left\| \nabla_{\mathbf{x}} \log \left(\frac{D(\mathbf{x})}{1 - D(\mathbf{x})} \right) \right\|_2^2 \right) \end{aligned}$$

Update the generator's parameters using an Adam optimizer with learning rate η and descending the gradient:

$$\nabla_{\theta_G} \left(\frac{1}{B} \sum_{i=1}^B \ell_\alpha(0, D(G(\mathbf{z}_i))) \right)$$

end for

Algorithm 2 Overview of Lk-SLkGAN training

Require k , Number of epochs n_e , Batch size B , Learning rate η
Initialize Generator G with parameters θ_G , Discriminator D with parameters θ_D .
for $i = 1$ to n_e **do**
 Sample batch of real data $\mathbf{x} = \{\mathbf{x}_1, \dots, \mathbf{x}_B\}$ from dataset
 Sample batch of Gaussian noise vectors $\mathbf{z} = \{\mathbf{z}_1, \dots, \mathbf{z}_B\} \sim \mathcal{N}(\mathbf{0}, \mathbf{I})$
 Update the discriminator's parameters using an Adam optimizer with learning rate η by descending the gradient:

$$\nabla_{\theta_D} \left(\frac{1}{B} \sum_{i=1}^B \left(\frac{1}{2} (D(\mathbf{x}_i) - 1)^2 + \frac{1}{2} (D(G(\mathbf{z}_i)))^2 \right) \right)$$

or **update** the discriminator's parameters with a simplified GP:

$$\begin{aligned} & \nabla_{\theta_D} \left(\frac{1}{B} \sum_{i=1}^B \left(\frac{1}{2} (D(\mathbf{x}_i) - 1)^2 + \frac{1}{2} (D(G(\mathbf{z}_i)))^2 \right) \right) \\ & + 5 \left(\sum_{i=1}^B \left\| \nabla_{\mathbf{x}} \log \left(\frac{D(\mathbf{x})}{1 - D(\mathbf{x})} \right) \right\|_2^2 \right) \end{aligned}$$

Update the generator's parameters using an Adam optimizer with learning rate η and descending the gradient:

$$\nabla_{\theta_G} \left(\frac{1}{B} \sum_{i=1}^B \frac{1}{2} (|1 - D(G(\mathbf{z}_i)))^k - 1) \right)$$

end for

Algorithm 3 Overview of Vanilla-SLkGAN training

Require k , Number of epochs n_e , Batch size B , Learning rate η

Initialize Generator G with parameters θ_G , Discriminator D with parameters θ_D .

for $i = 1$ to n_e **do**

Sample batch of real data $\mathbf{x} = \{\mathbf{x}_1, \dots, \mathbf{x}_B\}$ from dataset

Sample batch of noise vectors $\mathbf{z} = \{\mathbf{z}_1, \dots, \mathbf{z}_B\} \sim \mathcal{N}(\mathbf{0}, \mathbf{I})$

Update the discriminator's parameters using an Adam optimizer with learning rate η by descending the gradient:

$$\nabla_{\theta_D} \left(-\frac{1}{B} \sum_{i=1}^B (\log(D(\mathbf{x}_i)) + \log(1 - D(G(\mathbf{z}_i)))) \right)$$

or **update** the discriminator's parameters with a simplified (GP):

$$\begin{aligned} \nabla_{\theta_D} \left(-\frac{1}{B} \sum_{i=1}^B (\log(D(\mathbf{x}_i)) + \log(1 - D(G(\mathbf{z}_i)))) \right) \\ + 5 \left(\sum_{i=1}^B \left\| \nabla_{\mathbf{x}} \log \left(\frac{D(\mathbf{x})}{1 - D(\mathbf{x})} \right) \right\|_2^2 \right) \end{aligned}$$

Update the generator's parameters using an Adam optimizer with learning rate η and descending the gradient:

$$\nabla_{\theta_G} \left(\frac{1}{B} \sum_{i=1}^B \frac{1}{2} (|1 - D(G(\mathbf{z}_i))|^k - 1) \right)$$

end for

References

- [1] S. M. Ali and S. D. Silvey. A general class of coefficients of divergence of one distribution from another. *Journal of the Royal Statistical Society. Series B (Methodological)*, 28(1):131–142, 1966.
- [2] Suguru Arimoto. Information-theoretical considerations on estimation problems. *Information and Control*, 19(3):181–194, 1971.
- [3] Martin Arjovsky, Soumith Chintala, and Léon Bottou. Wasserstein Generative Adversarial Networks. In *International Conference on Machine Learning*, pages 214–223. PMLR, 2017.
- [4] Himesh Bhatia, William Paul, Fady Alajaji, Bahman Ghahsifard, and Philippe Burlina. Least kth-order and Rényi generative adversarial networks. *Neural Computation*, 33(9):2473–2510, 2021.
- [5] Imre Csiszar. Eine Informationstheoretische Ungleichung und ihre Anwendung auf den Beweis der Ergodizität von Markoffschen Ketten. *Publications of the Mathematical Institute of the Hungarian Academy of Sciences, Series A*, 8, 01 1963.
- [6] Imre Csiszár. Information-type measures of difference of probability distributions and indirect observations. *Studia Sci. Math. Hungarica*, 2:299–318, 1967.
- [7] Li Deng. The MNIST Database of Handwritten Digit Images for Machine Learning Research [Best of the Web]. *IEEE Signal Processing Magazine*, 29(6):141–142, 2012.
- [8] Ian Goodfellow, Jean Pouget-Abadie, Mehdi Mirza, Bing Xu, David Warde-Farley, Sherjil Ozair, Aaron Courville, and Yoshua Bengio. Generative Adversarial Nets. In Z. Ghahramani, M. Welling, C. Cortes, N. Lawrence, and K.Q. Weinberger, editors, *Advances in Neural Information Processing Systems*, volume 27, pages 2672–2680. Curran Associates, Inc., 2014.
- [9] Ishaan Gulrajani, Faruk Ahmed, Martin Arjovsky, Vincent Dumoulin, and Aaron C Courville. Improved Training of Wasserstein GANs. *Advances in Neural Information Processing Systems*, 30, 2017.
- [10] E. Hellinger. *Journal für die reine und angewandte Mathematik*, 1909(136):210–271, 1909.
- [11] Martin Heusel, Hubert Ramsauer, Thomas Unterthiner, Bernhard Nessler, and Sepp Hochreiter. GANs trained by a two time-scale update rule converge to a local Nash equilibrium. In *Advances in Neural Information Processing Systems*, pages 6626–6637, 2017.
- [12] James Jordon, Jinsung Yoon, and Mihaela Van Der Schaar. PATE-GAN: Generating synthetic data with differential privacy guarantees. In *Proceedings of the International Conference on Learning Representations*, 2018.

- [13] Diederik Kingma and Jimmy Ba. Adam: A Method for Stochastic Optimization. In *Proceedings of the International Conference on Learning Representations*, 2014.
- [14] Alex Krizhevsky, Geoffrey Hinton, et al. Learning multiple layers of features from tiny images. 2009.
- [15] Solomon Kullback and Richard A Leibler. On Information and Sufficiency. *The Annals of Mathematical Statistics*, 22(1):79–86, 1951.
- [16] Gowtham R Kurri, Tyler Sypherd, and Lalitha Sankar. Realizing GANs via a tunable loss function. In *Proceedings of the IEEE Information Theory Workshop (ITW)*, pages 1–6, 2021.
- [17] Gowtham R Kurri, Monica Welfert, Tyler Sypherd, and Lalitha Sankar. α -GAN: Convergence and estimation guarantees. In *Proceedings of the IEEE International Symposium on Information Theory (ISIT)*, pages 276–281, 2022.
- [18] Yong-Hoon Kwon and Min-Gyu Park. Predicting Future Frames Using Retrospective Cycle GAN. In *Proceedings of the IEEE/CVF Conference on Computer Vision and Pattern Recognition (CVPR)*, June 2019.
- [19] F. Liese and I. Vajda. On Divergences and Informations in Statistics and Information Theory. *IEEE Transactions on Information Theory*, 52(10):4394–4412, 2006.
- [20] Zinan Lin, Ashish Khetan, Giulia Fanti, and Sewoong Oh. PacGAN: The power of two samples in generative adversarial networks. In S. Bengio, H. Wallach, H. Larochelle, K. Grauman, N. Cesa-Bianchi, and R. Garnett, editors, *Advances in Neural Information Processing Systems*, volume 31. Curran Associates, Inc., 2018.
- [21] Xudong Mao, Qing Li, Haoran Xie, Raymond Y.K. Lau, Zhen Wang, and Stephen Paul Smolley. Least Squares Generative Adversarial Networks. In *Proceedings of the IEEE International Conference on Computer Vision (ICCV)*, Oct 2017.
- [22] Frank Nielsen. On a generalization of the Jensen–Shannon divergence and the Jensen–Shannon centroid. *Entropy*, 22(2):221, 2020.
- [23] Frank Nielsen and Richard Nock. On the chi square and higher-order chi distances for approximating f-divergences. *IEEE Signal Processing Letters*, 21(1):10–13, 2013.
- [24] Sebastian Nowozin, Botond Cseke, and Ryota Tomioka. f-gan: Training generative neural samplers using variational divergence minimization. *Advances in Neural Information Processing Systems*, 29, 2016.

- [25] Ferdinand Österreicher. On a class of perimeter-type distances of probability distributions. *Kybernetika*, 32(4):389–393, 1996.
- [26] Xingang Pan, Xiaohang Zhan, Bo Dai, Dahua Lin, Chen Change Loy, and Ping Luo. Exploiting deep generative prior for versatile image restoration and manipulation. *IEEE Transactions on Pattern Analysis and Machine Intelligence*, 44(11):7474–7489, 2021.
- [27] Alec Radford, Luke Metz, and Soumith Chintala. Unsupervised Representation Learning with Deep Convolutional Generative Adversarial Networks. In *Proceedings of the 9th International Conference on Image and Graphics*, pages 97–108, 2017.
- [28] Alfréd Rényi. On measures of entropy and information. In *Proceedings of the Fourth Berkeley Symposium on Mathematical Statistics and Probability, Volume 1: Contributions to the Theory of Statistics*, volume 4, pages 547–562. University of California Press, 1961.
- [29] Igal Sason. On f-Divergences: Integral Representations, Local Behavior, and Inequalities. *Entropy*, 20(5):383, May 2018.
- [30] Tim Van Erven and Peter Harremoës. Rényi divergence and Kullback-Leibler divergence. *IEEE Transactions on Information Theory*, 60(7):3797–3820, 2014.
- [31] Monica Welfert, Kyle Otstot, Gowtham R Kurri, and Lalitha Sankar. (α_D, α_G) -GANs: Addressing GAN Training Instabilities via Dual Objectives. In *Proceedings of the IEEE International Symposium on Information Theory (ISIT)*, 2023.